Enabling Directional Frequency-Selective Power Transmission in Ultrasonic Guided Wave Inspections

Enabling Directional Frequency-Selective Power Transmission in Ultrasonic Guided Wave Inspections

Masoud Mohammadgholiha
DEI - University of Bologna
40136 Bologna, Italy
m.mohammadgholiha@unibo.it

Stefano Taccetti
ARCES - University of Bologna
40136 Bologna, Italy
stefano.taccetti2@unibo.it

Luca De Marchi
DEI - University of Bologna
40136 Bologna, Italy
l.demarchi@unibo.it

***Abstract*—In this paper, an Ultrasonic Wireless Power Transfer system is introduced, featuring a novel piezoelectric transducer called the Frequency-Steerable Acoustic Transducer (FSAT). The focus is on utilizing FSAT's directional properties for efficient power transmission via ultrasonic guided waves, particularly suited for supplying power to inaccessible sensor nodes in structural health monitoring applications. Through finite element simulations and experimental tests, the power transfer process is analyzed, investigating the relationship between transmission frequency, transmitted and received voltage, and power efficiency. Furthermore, comparative evaluations with traditional piezoelectric transducers are conducted, both through FE simulations and experimental tests. The results highlight the superior performance of FSAT for ultrasonic wireless power transfer applications by achieving over 16 times higher voltage using FSAT than traditional piezoelectric transducers.**

***Index Terms*—Guided waves, frequency steerable acoustic transducers (FSATs)**

I. Introduction

Structural health monitoring (SHM) and nondestructive evaluation (NDE) using Ultrasonic Guided Waves (GWs) have garnered significant attention owing to GWs' ability to travel long distances across a structure with little attenuation [1], [2]. Beyond traditional applications, GWs are increasingly explored for ultrasonic wireless power transfer (WPT) to energize inaccessible sensor nodes and mitigate battery replacement costs [3]. Moreover, this requirement becomes crucial in metal structures monitoring applications (e.g., fuselages, containers, or chassis), where perforations for supply wires can compromise structural integrity [4].

For these reasons, WPT can be considered an alternative or additional solution to typical energy harvesting techniques, such as thermal or vibrational, that are affected by problems of time and space availability of the natural energy source [5]. This approach addresses issues associated with inductive WPT, such as the metal shielding effect in standard materials [6].

In fact, the energy harvested during the inspection phase by advanced actuation-transduction solutions can power smart sensor nodes directly attached to the components. This enables on-board processing and outsourcing of inspection results [7].

In general, the active ultrasonic inspection system can be implemented using multiple piezoelectric (PZT) transducers arranged and permanently attached to the structure being inspected [8]. However, this approach faces significant challenges such as weight penalties, intricate circuitry, and maintenance issues linked to extensive wiring.

This study explores the potential of Frequency Steerable Acoustic Transducers (FSATs) with inherent directional capabilities as an alternative to conventional PZT transducers, aiming to simplify hardware, reduce costs, and overcome existing challenges [9]–[11]. FSATs leverage frequency-dependent spatial filtering effects, resulting in a direct correlation between the direction of propagation and the frequency content of the transmitted/received signals. Therefore, beam steering/focusing can be achieved by controlling the central frequency of actuation and it is performed by a single transducer, instead of an array of PZTs, significantly reducing power consumption and the number of connecting cables.

In this work, a specific type of FSATs, termed Discrete-FSAT [12] was employed for directional transmission of GWs over a thin aluminum plate. This transducer is designed to actuate or sense the propagation of Lamb waves in three orientations using varying frequencies and has three channels with three distinct frequencies for each direction, ranging from 50 to $450\,\mathrm{kHz}$.

The study investigates the use of Discrete-FSATs for WPT, comparing their performance with traditional PZT transducers. The following section outlines simulations conducted to analyze ultrasonic WPT with these transducers, while the last part focuses on experimental procedures and their results.

II. Finite Element simulations

In this study, COMSOL Multiphysics software [13] was chosen to build a 3D finite element (FE) model of the proposed UWPT system, embedding structural mechanics, electrostatics, and electrical circuit physics to simulate the power conversion and transmission processes.

In order to have a direct comparison with the results of the available experimental setup, a system made up of two Discrete-FSATs bonded at a distance of $50\,\mathrm{cm}$ on a $1\,\mathrm{mm}$ thick

aluminum plate was simulated. Due to the inherent correlation between the propagation direction of ultrasonic waves and the orientation of the two transducers, three specific frequencies (50,83,123 kHz) were chosen. These frequencies correspond to the 0° direction, which connects the transmitter (TX) and receiver (RX) FSATs on the setup plate. This model was studied through frequency-domain simulations, as they are the fastest way to analyze the system behavior at the three mentioned frequencies.

Since the FSAT is accessible by a couple of channels and, when employed for transmission, the two channels' voltages need to be in phase opposition to perform the beam steering action, two continuous AC voltage supplies of 10 V amplitude and a phase shift of 180° were applied at the TX FSAT's electrodes. The receiver-side transducer (RX) is also accessible by two channels, that generate two voltages again in phase opposition. The differential output voltage of this second transducer, whose peak-to-peak value is approximately double that of each single channel, was then measured in an open-circuit situation. The same procedure was performed for the conventional PZT disc transducers for the sake of comparison, considering one single channel for the TX side and one single channel for the RX side.

The displacement wavefield at 123 kHz for two cases of FSAT and PZT disc is depicted respectively in Fig. 1 and Fig. 2. Results showcase the efficacy of FSATs in achieving excellent directional wave transmission, surpassing the omni-directional wave generation of conventional PZT transducers.

To assess the power transmission efficiency, the output power of the transmitter and receiver was determined as follows [4]:

$$P = \frac{U_{RMS}^2}{|Z|} \cdot \cos\theta \tag{1}$$

where U_{RMS} represents the effective voltage across the transducer, $|Z|$ indicates the modulus of the impedance of the FSAT, and θ represents the impedance angle. The transmission efficiency is compared at the three different frequencies, revealing the superior performance of the proposed FSAT device over conventional PZT discs for wireless power transmission, as displayed in Fig. 3.

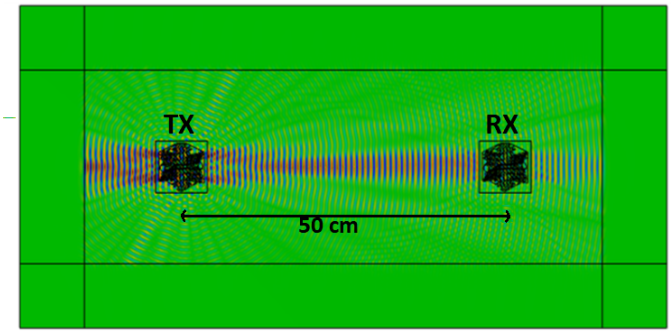

Fig. 1. COMSOL Discrete-FSAT displacement wavefield at 123 kHz

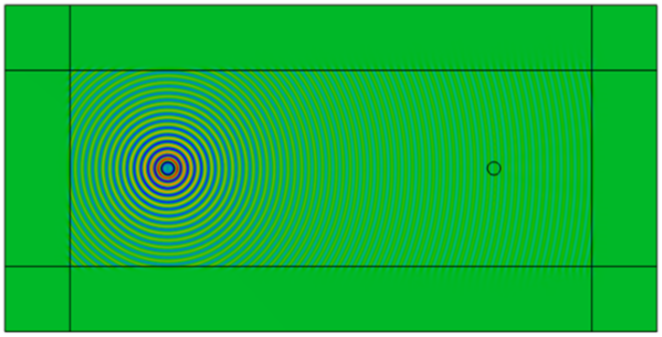

Fig. 2. COMSOL PZT displacement wavefield at 123 kHz

Finally, a set of finite element simulations in the frequency domain was conducted for the Discrete-FSAT model, to find the relationship between the differential voltage at the receiving end, transmission frequency, and voltage amplitude at the transmitting side. Fig. 4 shows values from this series of simulations, highlighting a linear relationship between voltage amplitude on TX and RX transducers' electrodes.

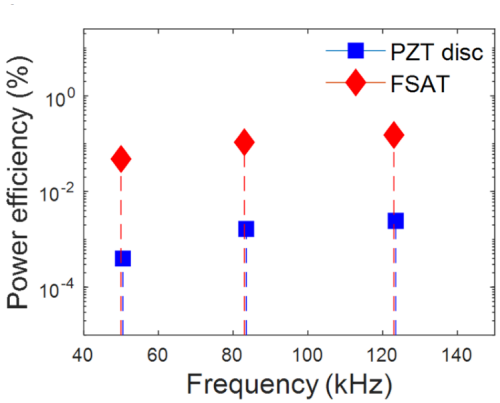

Fig. 3. Power efficiency comparison between PZT and Discrete-FSAT at 50,83,123 kHz from COMSOL AC simulations

III. Experiments and Results

Following the results obtained from the FE simulations, experimental tests were then carried out to compare performances of the two proposed systems at 50,83 and 123 kHz on a square aluminum plate with a length of 1 m and a thickness of 1 mm. A function generator (AFG31000,Tektronix) was used for generating continuous sinusoidal signals varying the voltage amplitude and the frequency between 50, 83 and 123 kHz. A power amplifier was introduced between the function generator and the transducer to reach higher peak-to-peak voltage values on the transmitter transducers' electrodes, obtaining a maximum value of 23 V peak-to-peak. Open circuit voltages at the receiving transducers' electrodes were finally measured using a digital multimeter (34401A, Agilent). Fig. 5 shows the experimental setup used for the Discrete-FSAT-based ultrasonic WPT system testing, with the transmitting and receiving transducers bonded on the aluminum plate.

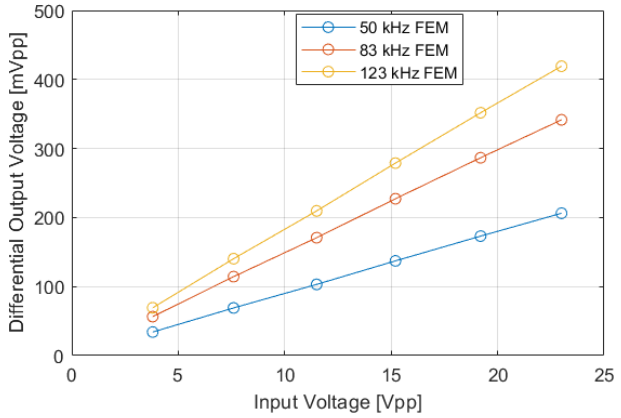

Fig. 4. COMSOL AC simulations: open circuit voltages received in a Discrete-FSAT-based WPT system at 50,83,123 kHz as a function of peak-to-peak amplitude on the transmitter FSAT

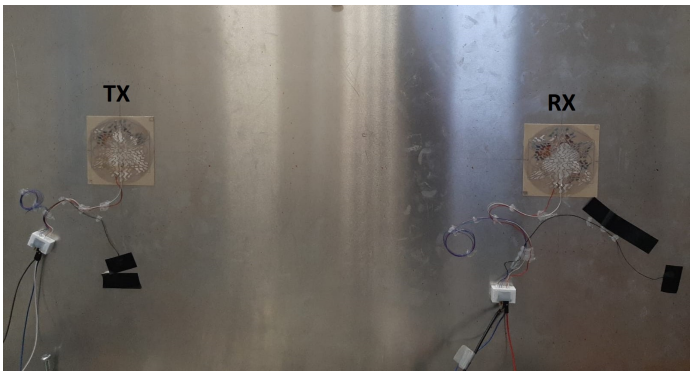

Fig. 5. Experimental setup: Discrete-FSAT bonded on the 1 mm thick aluminium plate, at a distance of 50 cm along the 0° direction

Fig. 6 shows the measured differential open circuit voltages at the receiving Discrete-FSAT electrodes, as a function of the transmission frequency and peak-to-peak voltage amplitude on the transmitter channels. These values point out a linear relationship between the voltage applied on the transmitter's electrodes and the one generated by the receiving transducer, as it was displayed by COMSOL simulations.

Finite Element simulation results and experimental values were then compared to check the correctness of the model for each of the three considered transmission frequencies. Fig. 7, to Fig. 9 respectively compare data from measurements and COMSOL simulations at 50, 83, and 123 kHz. Overall, test data validated the accuracy of the FE model. Discrepancies between simulation results and measurements stem from variations in conditions, including imperfect bonding of the transducer, variations in piezoelectric properties, and non-idealities in devices such as connection cable resistances and instrument impedances. Tests showed that system linearity reaches its maximum at 83 kHz transmissions, while the highest values of received open circuit voltage correspond to 123 kHz transmissions.

The same open circuit voltage measurements were made for

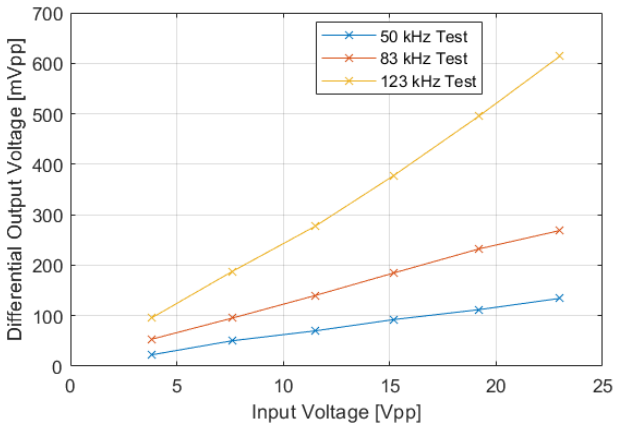

Fig. 6. Open circuit voltage received in a Discrete-FSAT-based WPT system at 50,83,123 kHz

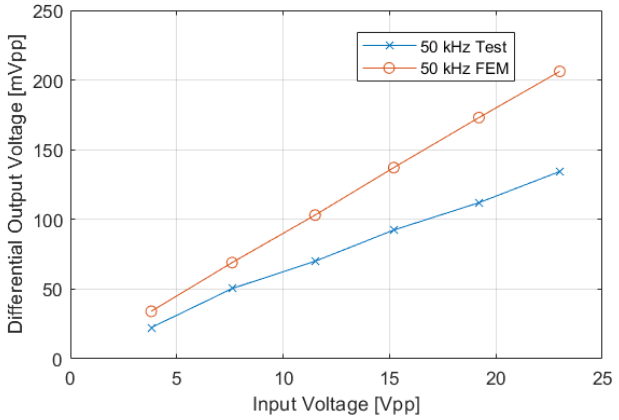

Fig. 7. Open circuit voltage received in a Discrete-FSAT-based WPT system at 50 kHz

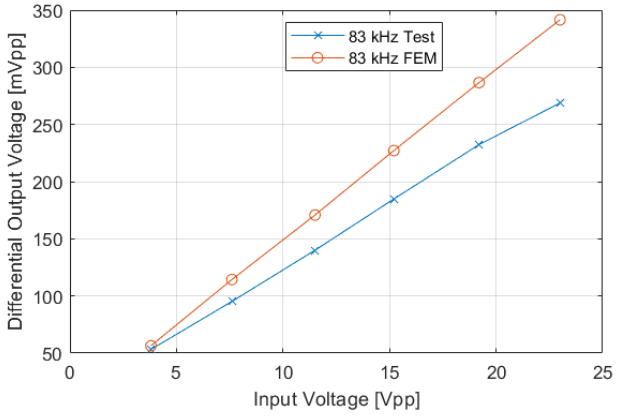

Fig. 8. Open circuit voltage received in a Discrete-FSAT-based WPT system at 83 kHz

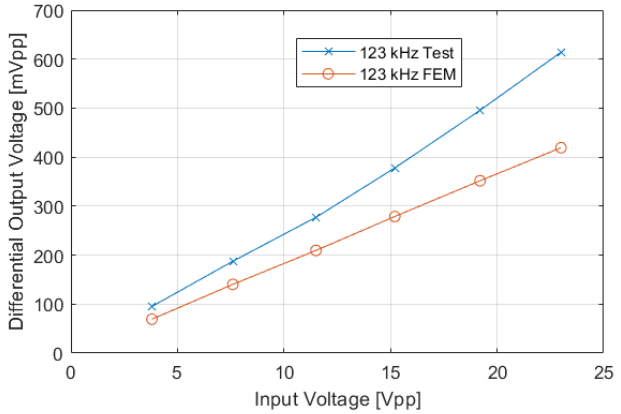

Fig. 9. Open circuit voltage received in a Discrete-FSAT-based WPT system at 123 kHz

a PZT-based wireless power transmission placing two Murata PZTs with a diameter of 2 cm at a distance of 50 cm on the same aluminum plate.

In order to compare the PZT performances with the Discrete-FSAT ones in the most meaningful condition, the PZT transmitter's single channel was excited with a 23 V peak-to-peak continuous sinusoidal voltage, and the receiving PZT's single channel open circuit voltage was measured.

Table I highlights the superior performances of a Discrete-FSAT-based WPT system over the PZT-based system, comparing the open circuit voltage values measured on the receiving transducers' electrodes of these two systems at the three different frequencies.

TABLE I
PZT-BASED SYSTEM AND FSAT-BASED SYSTEM TRANSMISSION TEST RESULTS WITH A DISTANCE OF 50 cm BETWEEN TRANSDUCERS AND A 23 V PEAK-TO-PEAK CONTINUOUS SINUSOIDAL VOLTAGE ON THE TX SIDE

Frequency [kHz]	PZT voltage [mVpp]	FSAT voltage [mVpp]
50	31.11	134.4
83	22.63	268.5
123	36.77	614.2

IV. Conclusions

In this work the problem of ultrasonic wireless power transfer was studied, both with traditional PZTs and with a novel kind of piezoelectric device, the Frequency Steerable Acoustic Transducer (FSAT). The FSAT's high directivity leads to better performances, in terms of transferred energy, compared with traditional omnidirectional PZTs, as shown by Finite Element simulations in COMSOL Multiphysics. Experimental tests proved the superiority of the FSAT over PZT for wireless power transfer applications. Indeed, considering the same conditions for the transmitter side, i.e. the same peak-to-peak voltage on the electrodes, and the same distance of 50 cm between TX and RX transducers on the aluminum plate, the Discrete-FSAT-based system revealed open circuit voltages at the receiving end over 16 times the ones measured in the PZT-based system. Experimental tests proved also the linear relationship between voltage amplitude on the transmitter side and voltage amplitude on the receiving transducers' electrodes. Applying two 23 V peak-to-peak continuous sinusoidal voltages in phase opposition on the two channels of the transmitting Discrete-FSATS at 50, 83, 123 kHz, differential open circuit voltages respectively of 134, 269 and 614 mV peak-to-peak were measured on the receiving FSAT, at the distance of 50 cm on a 1 mm thick aluminum plate.

Acknowledgment

The research was conducted as part of the Guided Waves for Structural Health Monitoring (GW4SHM) project, which is financially supported by the Marie Skłodowska-Curie Actions Innovative Training Network (Grant No. 860104).

References

[1] Moritz Mälzer, Christian Kexel, Thomas Maetz, and Jochen Moll. Combined inspection and data communication network for lamb-wave structural health monitoring. *IEEE Transactions on Ultrasonics, Ferroelectrics, and Frequency Control*, 66(10):1625–1633, 2019.

[2] Marco Dibiase, Masoud Mohammadgholiha, and Luca De Marchi. Optimal array design and directive sensors for guided waves doa estimation. *Sensors*, 22(3):780, 2022.

[3] Victor Farm-Guoo Tseng, Sarah S. Bedair, Joshua J. Radice, Trevon E. Drummond, and Nathan Lazarus. Ultrasonic lamb waves for wireless power transfer. *IEEE Transactions on Ultrasonics, Ferroelectrics, and Frequency Control*, 67(3):664–670, 2020.

[4] Yunfei Xu, Yongshun Sun, Jian Tang, Chao Wei, Xiaoxi Ding, and Wenbin Huang. A lamb waves-based wireless power transmission system for powering iot sensor nodes. *Smart Materials and Structures*, 31(10):105009, aug 2022.

[5] Aleksander Kural, Rhys Pullin, Karen Holford, Jonathan Lees, Jack Naylon, Christophe Paget, and Carol Featherston. Design and characterization of an ultrasonic lamb wave power delivery system. *IEEE Transactions on Ultrasonics Ferroelectrics and Frequency Control*, 60, 05 2013.

[6] Victor Farm-Guoo Tseng, Sarah S. Bedair, and Nathan Lazarus. Acoustic power transfer and communication with a wireless sensor embedded within metal. *IEEE Sensors Journal*, 18(13):5550–5558, 2018.

[7] Yongshun Sun, Yunfei Xu, Wei Li, Quanchang Li, Xiaoxi Ding, and Wenbin Huang. A lamb waves based ultrasonic system for the simultaneous data communication, defect inspection, and power transmission. *IEEE Transactions on Ultrasonics, Ferroelectrics, and Frequency Control*, 68(10):3192–3203, 2021.

[8] Lingyu Yu and Victor Giurgiutiu. In situ 2-d piezoelectric wafer active sensors arrays for guided wave damage detection. *Ultrasonics*, 48(2):117–134, 2008.

[9] Matteo Senesi and Massimo Ruzzene. A frequency selective acoustic transducer for directional lamb wave sensing. *The Journal of the Acoustical Society of America*, 130(4):1899–1907, 2011.

[10] Masoud Mohammadgholiha, Antonio Palermo, Nicola Testoni, Jochen Moll, and Luca De Marchi. Finite element modeling and experimental characterization of piezoceramic frequency steerable acoustic transducers. *IEEE Sensors Journal*, 22(14):13958–13970, 2022.

[11] Octavio A Márquez Reyes, Beata Zima, Jochen Moll, Masoud Mohammadgholiha, and Luca de Marchi. A numerical study on baseline-free damage detection using frequency steerable acoustic transducers. In *European Workshop on Structural Health Monitoring*, pages 24–33. Springer, 2022.

[12] Masoud Mohammadgholiha, Federica Zonzini, Jochen Moll, and Luca De Marchi. Directional multifrequency guided waves communications using discrete frequency-steerable acoustic transducers. *IEEE Transactions on Ultrasonics, Ferroelectrics, and Frequency Control*, 70(11):1494–1505, 2023.

[13] COMSOL AB. Comsol multiphysics v. 5.6,. Online, 2022.